Supplementary Figures

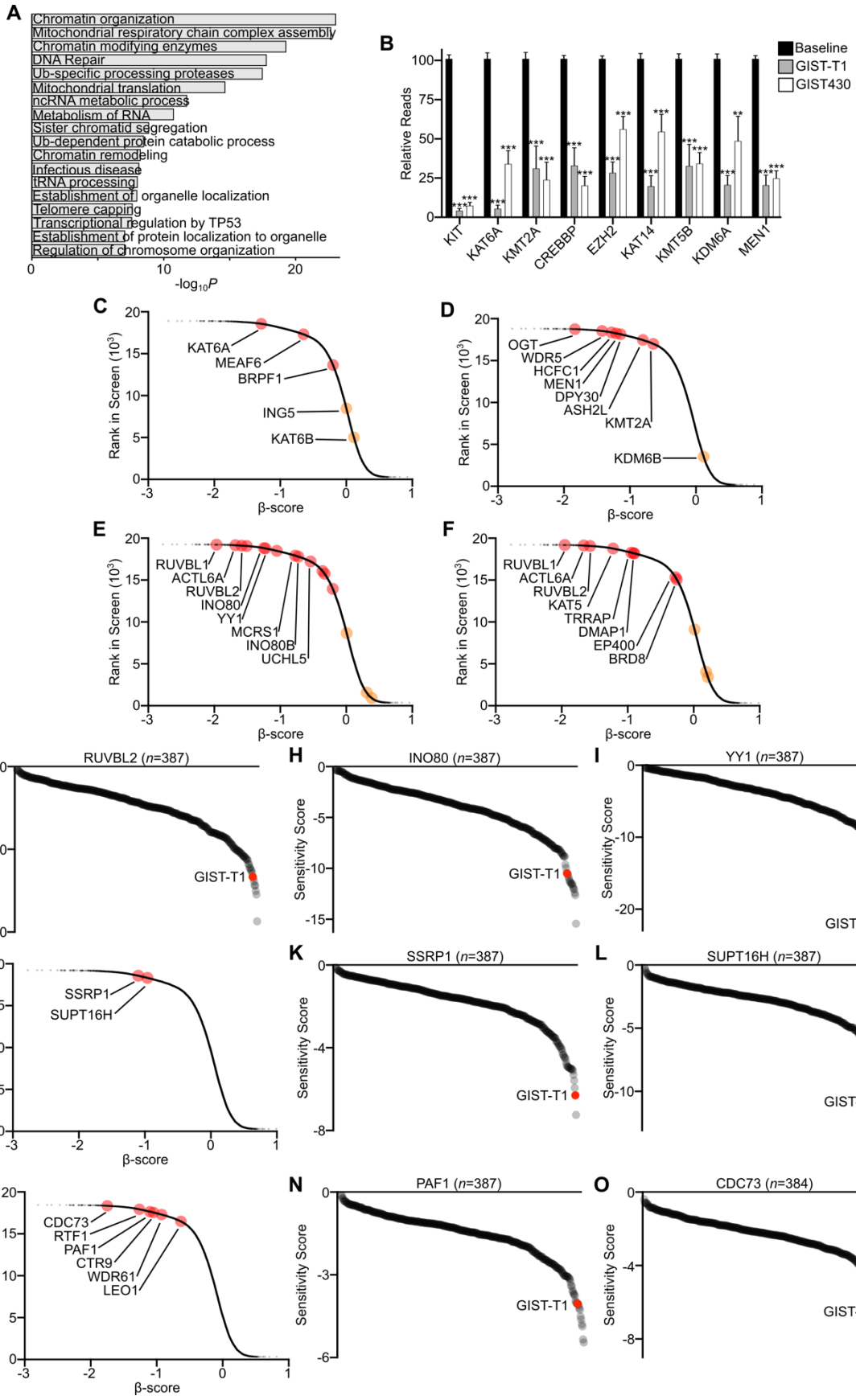
A
Chromatin organization
Mitochondrial respiratory chain complex assembly
Chromatin modifying enzymes
DNA Repair
Ub-specific processing proteases
Mitochondrial translation
ncRNA metabolic process
Metabolism of RNA
Sister chromatid segregation
Ub-dependent protein catabolic process
Chromatin remodeling
Infectious disease
tRNA processing
Establishment of organelle localization
Telomere capping
Transcriptional regulation by TP53
Establishment of protein localization to organelle
Regulation of chromosome organization
-log10P
B
Baseline
GIST-T1
GIST430
Relative Reads
KIT
KAT6A
KMT2A
CREBBP
EZH2
KAT14
KMT5B
KDM6A
MEN1
C
KAT6A
MEAF6
BRPF1
ING5
KAT6B
Rank in Screen (10³)
β-score
D
OGT
WDR5
HCFC1
MEN1
DPY30
ASH2L
KMT2A
KDM6B
E
RUVBL1
ACTL6A
RUVBL2
INO80
YY1
MCRS1
INO80B
UCHL5
F
RUVBL1
ACTL6A
RUVBL2
KAT5
TRRAP
DMAP1
EP400
BRD8
G
RUVBL2 (n=387)
Sensitivity Score
GIST-T1
H
INO80 (n=387)
I
YY1 (n=387)
J
SSRP1
SUPT16H
K
SSRP1 (n=387)
L
SUPT16H (n=387)
M
CDC73
RTF1
PAF1
CTR9
WDR61
LEO1
N
PAF1 (n=387)
O
CDC73 (n=384)

Figure S1. Unique GIST dependencies. **A,** Plot showing the top 18 significantly enriched gene ontology terms among genes uniquely essential to GIST. **B,** Relative reads for the top 8 sgRNAs targeting the indicated genes in GIST-T1 or GIST430, normalized to baseline plasmid library (*n*=2 per sgRNA). Data were analyzed by one-way ANOVA with Dunnett's multiple comparisons test, compared to Baseline; ***,*P*<0.001; **,*P*<0.01. **C**, Plot of rank in screen and β-score highlighting MOZ complex members and KAT6B as comparator; statistically significant β-scores are indicated in red, and non-significant in orange. **D,** Plot of rank in screen and β-score highlighting Menin-MLL complex members. **E,** Plot of rank in screen and β-score highlighting INO80 complex members. **F,** Plot of rank in screen and β-score highlighting NuA4 histone acetyltransferase complex members. **G-I,** Ranked Sensitivity Score from Project Drive cell lines (*n*=387) for select members of the INO80 and NuA4 complexes, with GIST-T1 highlighted in red. **J,** Plot of rank in screen and β-score highlighting FACT complex members. **K-L,** Ranked Sensitivity Score from Project Drive cell lines (*n*=387) for members of the FACT complex, with GIST-T1 highlighted in red. **M,** Plot of rank in screen and β-score highlighting PAF1 complex members. **N-O,** Ranked Sensitivity Score from Project Drive cell lines (*n*=387) for select members of the PAF1 complex, with GIST-T1 highlighted in red.

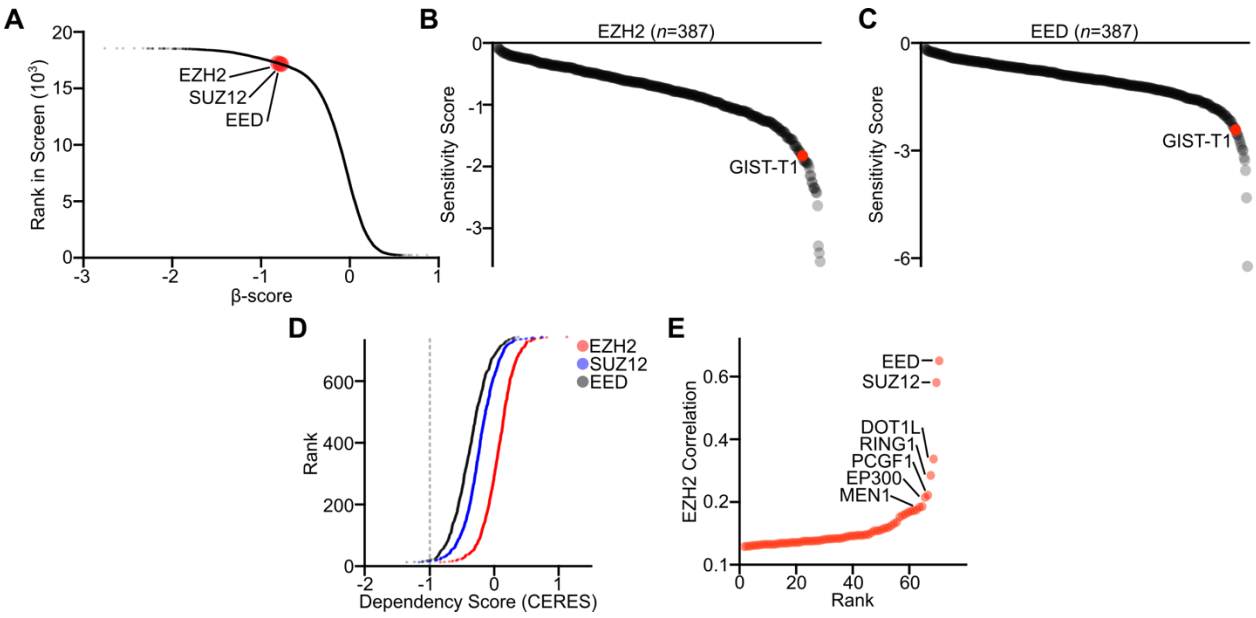

Figure S2. PRC2 complex dependency in GIST. **A,** Plot of rank in screen and β-score highlighting core PRC2 complex members. **B-C,** Ranked Sensitivity Score from Project Drive cell lines (*n*=387) for select members of the PRC2 complex, with GIST-T1 highlighted in red. **D,** Plot of rank and CERES dependency score for EZH2 complex members across DepMap cell lines (*n*=726), with the dotted line at -1 indicating significant dependency. **E,** Top 70 gene dependency correlations of EZH2 in DepMap. Co-dependent chromatin modifying enzymes and complex members are labeled.

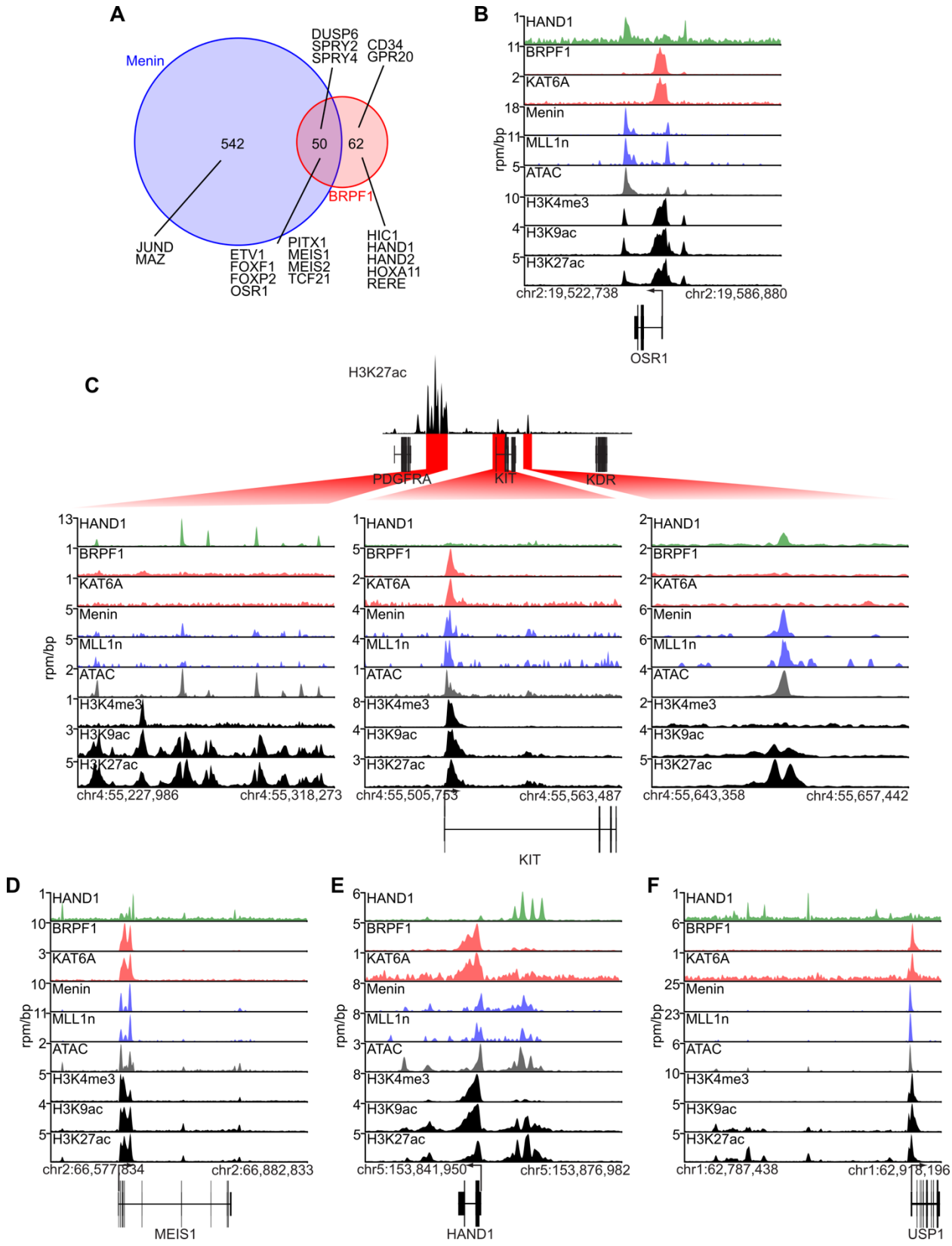
A
Menin
BRPF1
542
50
62
DUSP6
SPRY2
SPRY4
CD34
GPR20
JUND
MAZ
ETV1
FOXF1
FOXP2
OSR1
PITX1
MEIS1
MEIS2
TCF21
HIC1
HAND1
HAND2
HOXA11
RERE
B
HAND1
BRPF1
KAT6A
Menin
MLL1n
ATAC
H3K4me3
H3K9ac
H3K27ac
rpm/bp
chr2:19,522,738
chr2:19,586,880
OSR1
C
H3K27ac
PDGFRA
KIT
KDR
HAND1
BRPF1
KAT6A
Menin
MLL1n
ATAC
H3K4me3
H3K9ac
H3K27ac
rpm/bp
chr4:55,227,986
chr4:55,318,273
chr4:55,505,753
chr4:55,563,487
chr4:55,643,358
chr4:55,657,442
KIT
D
HAND1
BRPF1
KAT6A
Menin
MLL1n
ATAC
H3K4me3
H3K9ac
H3K27ac
rpm/bp
chr2:66,577,834
chr2:66,882,833
MEIS1
E
HAND1
BRPF1
KAT6A
Menin
MLL1n
ATAC
H3K4me3
H3K9ac
H3K27ac
rpm/bp
chr5:153,841,950
chr5:153,876,982
HAND1
F
HAND1
BRPF1
KAT6A
Menin
MLL1n
ATAC
H3K4me3
H3K9ac
H3K27ac
rpm/bp
chr1:62,787,438
chr1:62,9
8,196
USP1

Figure S3. Menin-MLL and MOZ complex localization in GIST. **A,** Overlap of enriched regions between Menin and BRPF1, with select GIST-associated genes indicated. **B-F**, Tracks showing regions of genomic occupancy of the TF HAND1, MOZ complex members BRPF1 and KAT6A, Menin-MLL complex members Menin and MLL1n and histone marks H3K4me3, H3K9ac and H3K27ac at the *OSR1*, *KIT*, *MEIS1*, *HAND1* and *USP1* loci.

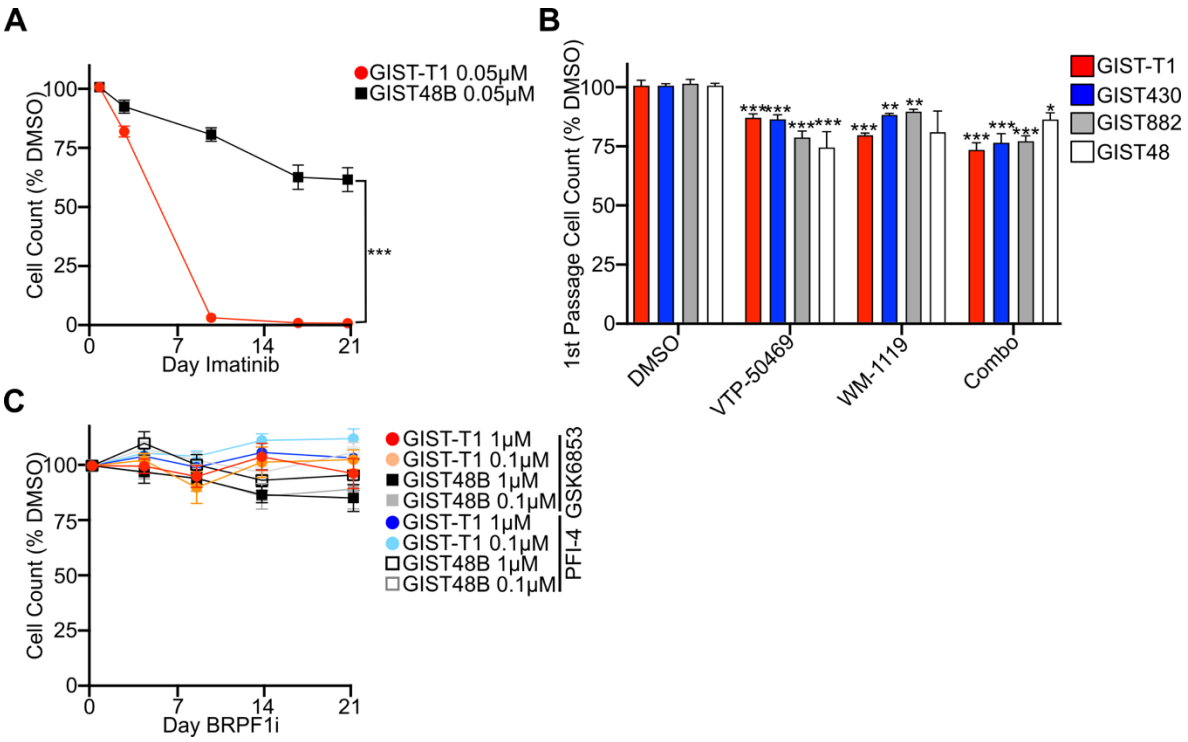

Figure S4. KAT6A, Menin and BRPF1 inhibition. **A,** Growth over time assay following treatment of GIST-T1 or GIST48B with 50 nM imatinib (*n*=5 per condition). Data were analyzed by two-way ANOVA, compared to GIST48B; ***,*P*<0.0001. **B**, DMSO-normalized cell count after the first passage of slowly growing GIST cell lines GIST430 (day 6), GIST882 (day 12) and GIST48 (day 12) in comparison to GIST-T1 (day 4). Cells were treated with VTP-50469 at 0.5 μM, WM-1119 at 1 μM or the combination with each drug at 0.1 μM (*n*=5-6 per condition). The first passage cell count was used to demonstrate on-target drug toxicity comparable to GIST-T1, as GIST882 and GIST48 cell lines replate poorly in this assay. Data were analyzed by one-way ANOVA with Dunnett's multiple comparisons test; compared to DMSO control ***,*P*<0.001; **,*P*<0.01; *,*P*<0.05. **C,** Growth over time assay treating GIST-T1 or GIST48B cells with selective BRPF1 inhibitors GSK6853 or PFI-4 at the indicated doses. No significant differences were observed by two-way ANOVA compared to DMSO control.

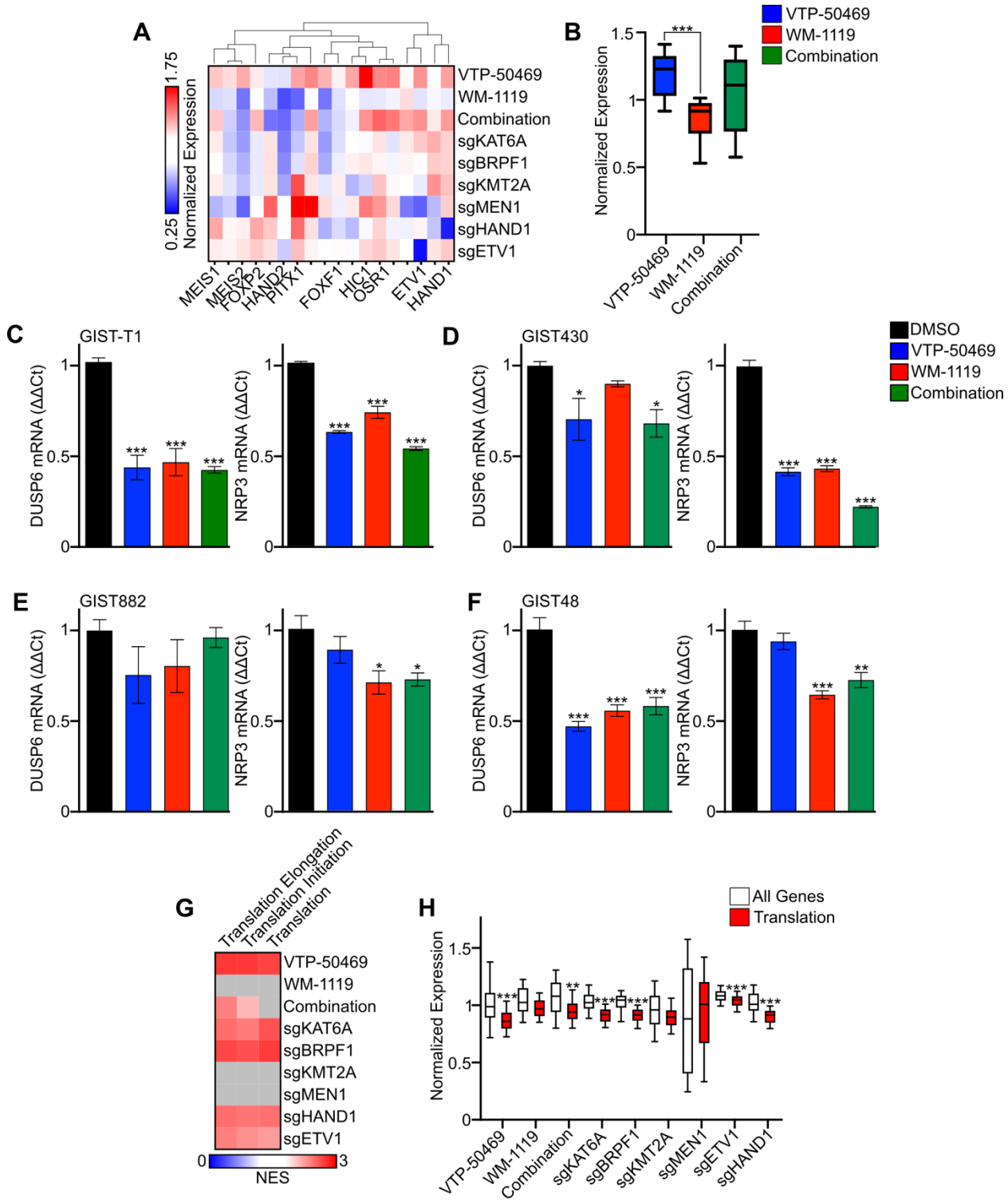
A
1.75
Normalized Expression
0.25
VTP-50469
WM-1119
Combination
sgKAT6A
sgBRPF1
sgKMT2A
sgMEN1
sgHAND1
sgETV1
MEIS1
MEIS2
FOXP2
HAND2
PITX1
FOXF1
HIC1
OSR1
ETV1
HAND1
B
VTP-50469
WM-1119
Combination
Normalized Expression
1.5
1
0.5
0
***
VTP-50469
WM-1119
Combination
C
GIST-T1
DUSP6 mRNA (ΔΔCt)
NRP3 mRNA (ΔΔCt)
D
GIST430
DMSO
VTP-50469
WM-1119
Combination
E
GIST882
F
GIST48
G
Translation Elongation
Translation Initiation
Translation
VTP-50469
WM-1119
Combination
sgKAT6A
sgBRPF1
sgKMT2A
sgMEN1
sgHAND1
sgETV1
0
3
NES
H
All Genes
Translation
Normalized Expression
VTP-50469
WM-1119
Combination
sgKAT6A
sgBRPF1
sgKMT2A
sgMEN1
sgETV1
sgHAND1

Figure S5. Transcriptional effects of MOZ and Menin disruption. **A,** Heatmap of control-normalized expression of GIST-associated TFs (10) in response to drug or sgRNA treatment. **B**, DMSO-normalized expression of 18 GIST-associated TFs in the indicated drug treatment (*n*=4 per condition). Data in were analyzed by one-way ANOVA with Tukey's multiple comparisons test, compared to VTP-50469; ***,*P*<0.001. **C**-**F**, Relative mRNA level by qRT-PCR of negative regulator of KIT signaling DUSP6 and HAND1- and SE-associated gene NPR3 in the indicated GIST cell lines treated for 5 days with VTP-50469 at 0.5 μM, WM-1119 at 1 μM or the combination with each drug at 0.1 μM (*n*=3-4 per group). Data in were analyzed by one-way ANOVA with Dunnett's multiple comparisons test, compared to DMSO; ***,*P*<0.001; **,*P*<0.01; *,*P*<0.05. **G**, Heatmap of GSEA data indicating the NES of Reactome translation-associated gene sets in each drug or sgRNA treatment condition. Only gene sets with significant FDRs are displayed using the color scale, with those bearing non-significant FDRs indicated in gray. **H**, Control-normalized expression of all translation-associated genes (*n*=48) in each sgRNA and drug treatment condition. Data were analyzed by Welch's *t* test, compared to All Genes; ***,*P*<0.001; **,*P*<0.01.

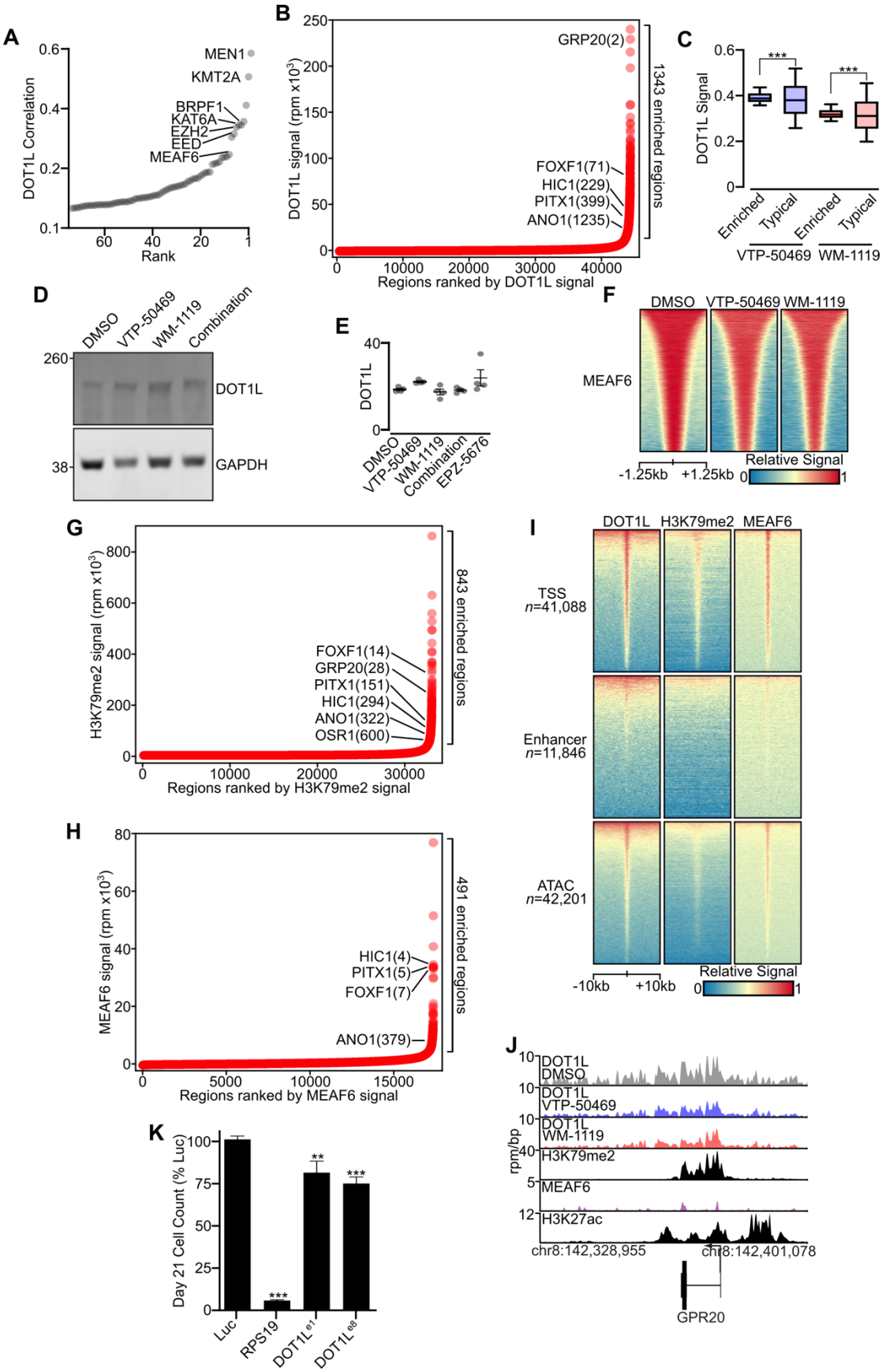
A
DOT1L Correlation
Rank
MEN1
KMT2A
BRPF1
KAT6A
EZH2
EED
MEAF6
B
DOT1L signal (rpm x10^3)
Regions ranked by DOT1L signal
GRP20(2)
FOXF1(71)
HIC1(229)
PITX1(399)
ANO1(1235)
1343 enriched regions
C
DOT1L Signal
***
Enriched
Typical
VTP-50469
WM-1119
D
DMSO
VTP-50469
WM-1119
Combination
DOT1L
GAPDH
E
DOT1L
EPZ-5676
F
MEAF6
Relative Signal
-1.25kb
+1.25kb
G
H3K79me2 signal (rpm x10^3)
Regions ranked by H3K79me2 signal
FOXF1(14)
GRP20(28)
PITX1(151)
HIC1(294)
ANO1(322)
OSR1(600)
843 enriched regions
H
MEAF6 signal (rpm x10^3)
Regions ranked by MEAF6 signal
HIC1(4)
PITX1(5)
FOXF1(7)
ANO1(379)
491 enriched regions
I
DOT1L
H3K79me2
MEAF6
TSS
n=41,088
Enhancer
n=11,846
ATAC
n=42,201
-10kb
+10kb
Relative Signal
J
DOT1L DMSO
DOT1L VTP-50469
DOT1L WM-1119
H3K79me2
MEAF6
H3K27ac
rpm/bp
chr8:142,328,955
chr8:142,401,078
GPR20
K
Day 21 Cell Count (% Luc)
Luc
RPS19
DOT1L e1
DOT1L e8

Figure S6. ChIP-seq of DOT1L, H3K79me2 and MEAF6 and effects of VTP-50469 and WM-1119. A, Top 70 gene dependency correlations of DOT1L in DepMap, with members of Menin-MLL, MOZ and PRC2 complex indicated. **B**, Enriched genomic regions of DOT1L binding. Select GIST-associated genes are indicated. **C**, DMSO-normalized signal for DOT1L in regions showing enriched (*n*=1,343) or typical (n=45,256) signal for DOT1L. Data were compared by Welch's *t* test; ***,*P*<0.001. **D**, Western blot showing DOT1L signal following 5 days of treatment with the indicated inhibitors. **E**, Levels of DOT1L expression by RNA-seq following 5 days of treatment with the indicated drugs; no significant changes were observed by one-way ANOVA with Dunnett's multiple comparisons test. **F**, Heat maps demonstrating spike-in normalized signal of MEAF6 at MACS-defined peaks (*n*=22,581) in GIST-T1 cells treated with DMSO, VTP-50469 or WM-1119. Scaled read densities ± 1.25 kb from the peak center are shown in rows. **G-H,** Enriched genomic regions of H3K79me2 and MEAF6 binding. Select GIST-associated genes are labeled. **I**, Heat maps demonstrating genomic localization in GIST-T1 of DOT1L, H3K79me2 and MEAF6 by ChIP-seq. Scaled read densities ± 10 kb from the TSS, H3K27ac-defined enhancers or ATAC-defined peaks are shown in rows. **J**, Tracks showing regions of genomic occupancy of spike-in normalized DOT1L under the indicated treatments, H3K79me2, MEAF6 and H3K27ac at the *GPR20* locus. **K**, Day 21 GIST-T1 cell count in a growth over time assay comparing sgRNAs targeting two DOT1L exons or Luc or RPS19 as control (*n*=5 per sgRNAs). Data were analyzed by one-way ANOVA with Dunnett's multiple comparisons test, compared to Luc control; ***,*P*<0.001; **,*P*<0.01.

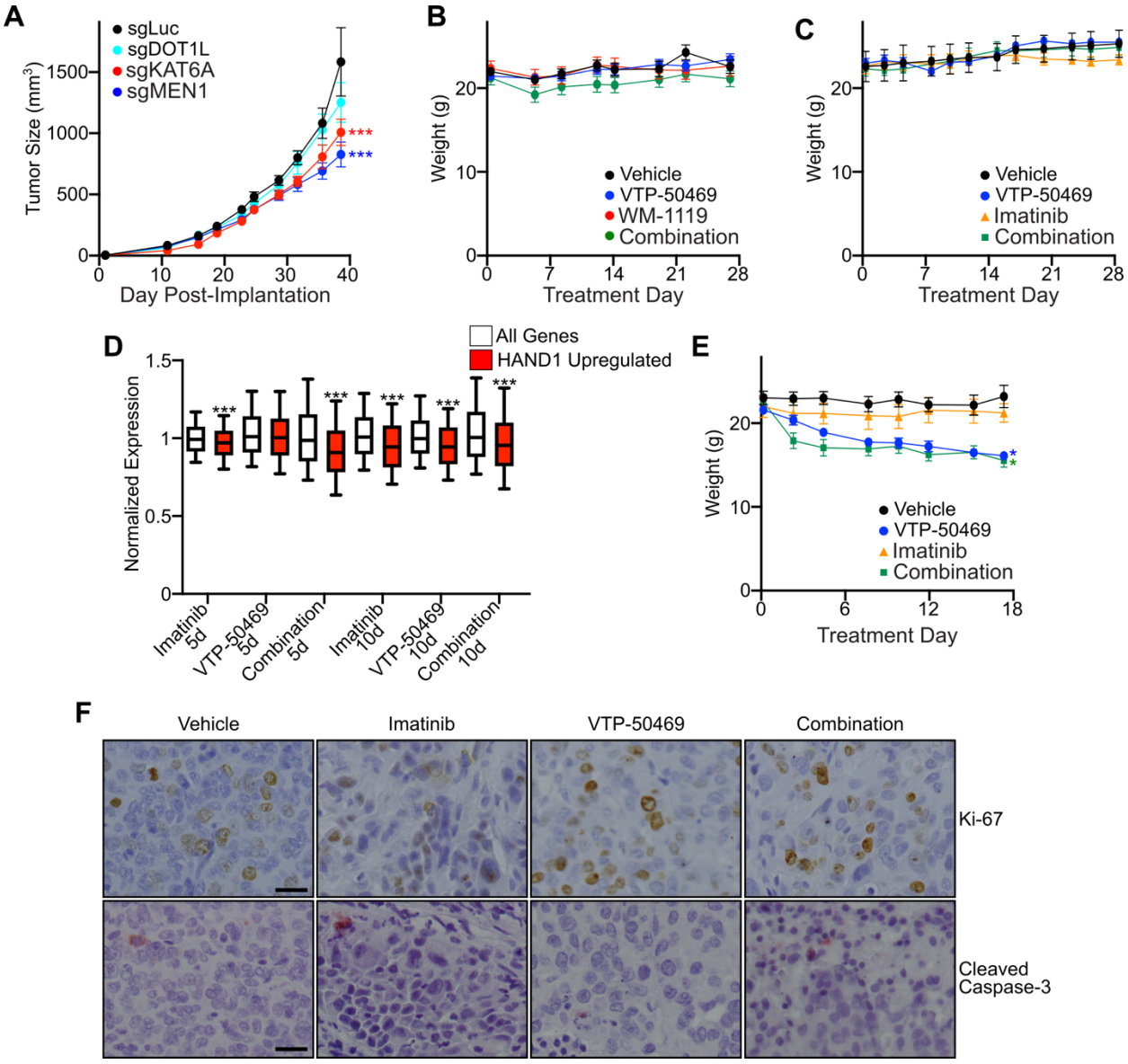
A
sgLuc
sgDOT1L
sgKAT6A
sgMEN1
Tumor Size (mm3)
Day Post-Implantation
***
***
B
Weight (g)
Vehicle
VTP-50469
WM-1119
Combination
Treatment Day
C
Weight (g)
Vehicle
VTP-50469
Imatinib
Combination
Treatment Day
D
All Genes
HAND1 Upregulated
Normalized Expression
Imatinib 5d
VTP-50469 5d
Combination 5d
Imatinib 10d
VTP-50469 10d
Combination 10d
E
Weight (g)
Vehicle
VTP-50469
Imatinib
Combination
Treatment Day
F
Vehicle
Imatinib
VTP-50469
Combination
Ki-67
Cleaved Caspase-3

Figure S7. Effects of sgRNA or drug treatment *in vivo*. **A**, GIST-T1/Cas9 cells were stably transduced with the indicated sgRNA, selected with puromycin *in vitro* for 14 days, and identical numbers of cells implanted and monitored for growth (n=10 tumors per group). Data were analyzed by two-way ANOVA, compared to sgLuc; ***,P<0.001. **B**, Weight of mice engrafted with the GIST-T1 cell line and treated for 28 days with WM-1119 (50 mg/kg gavage three times per day, 7d/week; n=6), VTP-50469 (0.1% in chow; n=5), combination WM-1119 and VTP-50469 (n=6) or vehicle control (n=5). **C,** Weight of mice engrafted with the GIST-T1 cell line and treated for 28 days with imatinib (50 mg/kg gavage 5d/week; n=5), VTP-50469 (0.1% in chow; n=4), combination imatinib and VTP-50469 (n=5) or vehicle control (n=5). **D**, Control-normalized expression of all expressed genes (n=7,434) or those whose expression is upregulated by HAND1 (n=438) in each treatment group. Data were analyzed by Welch's t test, compared All Genes; ***,P<0.001; **,P<0.01; *,P<0.05. **E,** Weight of mice engrafted with the PG27 PDX and treated for 18 days with imatinib (50 mg/kg gavage 5d/week; n=5), VTP-50469 (0.1% in chow; n=5), combination imatinib and VTP-50469 (n=5) or vehicle control (n=5). Data were analyzed by two-way ANOVA, compared to vehicle; *,P<0.05. **F,** PG27 tumors were harvested at the end of the treatment period and fixed tissues sectioned and evaluated for Ki-67 (top row) and cleaved caspase-3 (bottom row); scale bar = 25μm.

Table S1. Genome-scale CRISPR screen. Columns indicate gene name, β-score, P-value and FDR.

Table S2. MEAF6 proximal proteins identified by BioID.

Table S3. Oligonucleotide sequences.

Table S4. Tumor Measurements.